Available online at www.sciencedirect.com

ScienceDirect

journal homepage: www.elsevier.com/locate/he

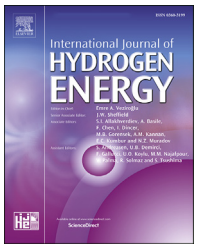

Steam gasification of Greek lignite and its chars by co-feeding CO_2 toward syngas production with an adjustable H_2/CO ratio

Athanasios Lampropoulos [a], *Vassilios Binas* [b], *Michalis Konsolakis* [c,**], *George E. Marnellos* [a,d,*]

[a] *University of Western Macedonia, Department of Mechanical Engineering, Kozani, Greece*
[b] *Foundation for Research and Technology-Hellas, Institute of Electronic Structure and Laser, Heraklion, Greece*
[c] *Technical University of Crete, School of Production Engineering and Management, Chania, Greece*
[d] *Centre for Research & Technology Hellas, Chemical Process & Energy Resources Institute, Thessaloniki, Greece*

HIGHLIGHTS

- Steam gasification of low rank Greek lignite (LG) and its chars was explored.
- Chars showed improved textural properties, higher fixed carbon and alkali index than raw LG.
- Slowly pyrolyzed chars exhibited higher carbon conversion and syngas yield.
- A close relationship between the syngas yield and the physicochemical properties was disclosed.
- The H_2/CO ratio can be suitably adjusted by co-feeding H_2O and CO_2 as gasifying agents.

ARTICLE INFO

Article history:
Received 20 March 2021
Received in revised form
30 May 2021
Accepted 14 June 2021
Available online 14 July 2021

Keywords:
Greek lignite
Lignite chars
Torrefaction
Slow pyrolysis
Combined steam and dry gasification
Syngas production

ABSTRACT

Low-rank lignite is among the most abundant and cheap fossil fuels, linked, however, to serious environmental implications when employed as feedstock in conventional thermoelectric power plants. Hence, toward a low-carbon energy transition, the role of coal in world's energy mix should be reconsidered. In this regard, coal gasification for synthesis gas generation and consequently through its upgrade to a variety of value-added chemicals and fuels constitutes a promising alternative. Herein, we thoroughly explored for a first time the steam gasification reactivity of Greek Lignite (LG) and its derived chars obtained by raw LG thermal treatment at 300, 500 and 800 °C. Moreover, the impact of CO_2 addition on H_2O gasifying agent mixtures was also investigated. Both the pristine and char samples were fully characterized by various physicochemical techniques to gain insight into possible structure-gasification relationships. The highest syngas yield was obtained for chars derived after LG thermal treatment at 800 °C, due mainly to their high content in fixed carbon, improved textural properties and high alkali index. Steam gasification of lignite and char samples led to H_2-rich syngas mixtures with a H_2/CO ratio of approximately 3.8. However, upon co-feeding CO_2 and H_2O, the H_2/CO ratio can be suitably adjusted for several potential downstream processes.

* *Corresponding author*. University of Western Macedonia, Department of Mechanical Engineering, Kozani, Greece.
** *Corresponding author*.
E-mail addresses: mkonsol@pem.tuc.gr (M. Konsolakis), gmarnellos@uowm.gr (G.E. Marnellos).
https://doi.org/10.1016/j.ijhydene.2021.06.131

Introduction

When the Paris Agreement for climate change was signed in 2015, coal demand was in the midpoint of a three year decline [1]. Various issues, such as the competition from renewable energy sources and natural gas along with the intergovernmental policies for a clean energy transition, are continuously narrowing the role of coal in world's energy mix. Currently coal amounts to ca. 28% share of global primary energy consumption and almost 40% of electricity generation with future projections, however, pointing out the importance of coal for power generation in developing countries and for the "more energy" scenario [2].

The ambitious Green Deal Strategy has been recently launched by the European Commission, to render Europe the first carbon neutral continent in 2050. In this direction, 42 regions in EU, including the Western Macedonia region, Greece, have to gradually abandon coal activities. Low rank lignite coal amounts to ca. 45% of coal recoverable reserves in the word [1], constituting the dominant domestic fossil fuel in Greece for more than six decades [3]. Even nowadays, lignite still holds a very high share in electricity production in Greece accounted for 30% in 2019 [3,4]. However, the steep phase out of coal without alternative strategies to effectively diversify the regional economy will result to serious socio-economic implications, as revealed by the recent study of Karasmanaki et al. [5].

In the above context, several strategies have been proposed for a just energy transition that are linked with the continuation of lignite reserves exploitation either for non-energy uses or by employing more energy efficient processes. In this regard, the Academy of Athens, in the report for the forthcoming post-lignite era in Greece, pointed out the importance of an alternative energy conversion route for lignite involving its gasification to syngas [6]. Syngas comprises a major building block for several commercially important chemicals (e.g., ammonia, methanol) and synthetic fuels (synthetic natural gas, Fischer-Tropsch liquid fuels) as well as an environmental friendly feedstock for power generation in gas turbines, internal combustion engines (ICEs), and fuel cells (e.g., SOFCs, MCFCs) [7–15].

The conventional coal-to-electricity process through the Carnot limited Rankine thermal cycle exhibits low electrical efficiency (ca. 30–40%), associated in addition with large amounts of key air pollutants [4,16]. Hence, the effective utilization of low rank coals in alternative energy conversion processes, such as pyrolysis and gasification, is of great importance towards improving the fuel characteristics and energy efficiency [17,18].

Gasification is the main thermochemical process to convert solid fossil or bio-based fuels to synthesis gas by using an oxidant medium comprising of either sub-stoichiometric air/oxygen or H_2O or CO_2 or mixtures of the above constituents to effectively control the heat requirements of the process and the distribution of products in the generated syngas [19,20]. Coal gasification, as an endothermic process, is typically taking place at elevated temperatures, i.e., 700–1200 °C, resulting in a mixture involving primarily H_2, CO, CO_2 and CH_4 but also negligible amounts of light hydrocarbons and other impurities such as H_2S, NH_3, HCN, etc, along with tars (vapors of condensed hydrocarbons) diluted in syngas and a solid residue consisting of chars and the inorganic matter of solid fuel feedstock [21]. As a complex physicochemical process, the gasification efficiency and syngas composition are strongly dependent on the fuel characteristics and employed operational conditions such as temperature, gasifying agent, heating rate, residence time, etc. [19,22,23].

The physicochemical characteristics of coals (e.g., fixed carbon, volatile matter, porosity, moisture, ash, etc) are crucial properties in defining gasification performance. Lignite coals are characterized by higher porosity compared to other bituminous coals, and thus are more suitable as fuel feedstock in the gasification process [10,24–26]. Torrefaction at low temperatures and slow pyrolysis at medium and high temperatures of pristine coals under inert atmospheres offer the opportunity to obtain chars with better characteristics as fuel feedstock in gasification. The produced chars exhibit higher energy density and porosity compared to pristine coals attributed to the devolatilization process and removal of contained moisture as well as to the rearrangement of the carbonaceous matter during thermal treatment [26–31].

The gasification operational conditions are also decisive factors for the overall process efficiency, i.e., how much of the chemical energy contained in the solid fuel is transformed into syngas [20]. Depending on the extent of the endothermic and exothermic reactions taking place during gasification, temperature significantly affects the carbon conversion and syngas composition [32]. In general, carbon conversion and H_2 and CO contents in synthesis gas are enhanced, while the amounts of CO_2, CH_4, hydrocarbons and tars are suppressed upon increasing the gasification temperature [19]. This behavior can be mainly attributed to the prevailing role of endothermic reactions at higher temperatures.

Syngas composition depends also strongly on the employed gasifying agent [33]. Although air gasification is among the most facile and economic technologies, the dilution by the N_2 (more than 50%) notably reduces the heating value of produced syngas [33]. On the other hand, steam gasification results in hydrogen-rich syngas mixtures, related, however, to high heat requirements [34,35]. CO_2 can be also considered as gasifying agent although has been more scarcely implemented. CO_2 interacts with carbon and generates almost exclusively CO, increasing carbon conversion efficiency, offering at the same time an alternative pathway to utilize industrial CO_2-captured emissions [36,37]. The combination of H_2O and CO_2 in gasifying agent mixtures at certain compositions can effectively manipulate the H_2/CO ratio in produced syngas according to its desired end uses.

Various studies have been dealing with the effect of coal thermal treatment [28,29,31,38,39] and the use of steam [38,40] or H_2O–CO_2 mixtures [41–46] as gasifying mediums on the overall gasification performance. For instance, Na Li et al. [28] reported on the gasification performance of Shengli lignite and its demineralized chars by employing steam as gasifying

agent. They observed that inherent minerals significantly reduced the ignition temperature of gasification, leading to higher H_2 production rates. They also noted that by increasing the thermal treatment of demineralized chars, higher syngas yields with increased H_2 contents can be obtained. This behavior was attributed to the formation of active catalytic complexes during the pyrolysis stage. J. Fermoso et al. [38] concluded that the increase in steam concentration during the gasification of five different rank coal chars led to an increase in their gasification reactivity. Sylvie Valin et al. [47] examined the influence of CO_2 as gasifying medium by totally or partially replacing steam during biomass gasification in a fluidised gasifier. The experimental tests revealed that the substitution of steam by CO_2 can adjust the H_2/CO ratio in syngas, meeting the required specifications for DME synthesis.

Relative works regarding the gasification of Greek lignite are quite rare [36,48,49]. Two of these studies report on the gasification of lignite employing CO_2 as gasification agent [36,48] and another one refers on its catalyst-aided hydrogasification [49]. A group at the National Technical University of Athens [18,50] elaborated a feasibility assessment on the air combined gasification of Greek lignite and solid waste in a case study focused on the region of Western Macedonia, Greece. Notably, there is no work in the existing literature investigating the steam gasification of Greek lignite and its derived chars through torrefaction or slow pyrolysis.

In the light of the above aspects, the present work originally explores the effect of Greek lignite thermal treatment protocols on the physicochemical characteristics of as-produced chars and their steam gasification efficiency in terms of carbon conversion, instant gasification rate, syngas production and composition. All fuel samples were physicochemically characterized by employing several methods including ultimate and proximate analysis, X-ray fluorescence (XRF), N_2 physisorption, Scanning Electron Microscopy/Energy Dispersive X-ray spectroscopy (SEM/EDX) and Fourier Transform Infrared (FTIR) spectroscopy to reveal possible relationships between the gasification performance of fuels and their physicochemical properties. Moreover, the impact of CO_2 as a co-gasifying medium on the gaseous products distribution and H_2/CO ratio in syngas was explored.

Experimental

Char production process

In the present work, lignite coal (LG) from the Western Macedonia basin, Greece, was selected as fuel. The procedure to obtain the chars at 300 °C (LG300), 500 °C (LG500) and 800 °C (LG800) has been described in detail elsewhere [51]. In brief, 75 gr of raw lignite (1–3 mm) were first inertized with pure nitrogen flow (500 cm^3/min) for 1 h and then thermally treated under a nitrogen atmosphere (250 cm^3/min, heating ramp 20 °C/min) up to the selected temperature (300, 500, and 800 °C for 1 h). The yields of the solid and liquid fractions were calculated by the weight of the solid residue and the condensed liquids after heat treatment. Permanent gases yield was calculated by the difference between the initial weight of pristine LG and the corresponding masses of solid and liquid fractions for each char.

Physicochemical characterization

All samples were characterized in terms of inorganic matter content (XRF), pore structure (BET method), surface morphology/composition (SEM/EDX), and structural properties (FTIR Spectroscopy), as described in detail elsewhere [51]. The chemical composition of fuel samples was determined in a Vario Macro CHN/CHNS analyzer for elemental analysis and in a TGA LECO 701 analyzer for proximate analysis.

Gasification experiments

The gasification experiments of pristine lignite (LG) and as-produced chars (LG300, LG500 and LG800) using either H_2O/He or H_2O/CO_2/He mixtures were performed in a fixed-bed reactor, loaded with 0.1 g of fuel. The experimental apparatus and the gasification reactor have been presented in detail elsewhere [51].

Initially, the fuels were exposed to an inert He flow of 30 cm^3 (STP)/min up to 300 °C (5 °C/min), where the feed was immediately switched to the selected gasifying mixture. The gasification experiments were carried out at 300–950 °C with a heating ramp of 2 °C/min. In the case of H_2O/He mixtures, pure He (Air Liquide) was flowing through a temperature-controlled saturator containing twice-distilled liquid water, and H_2O vapors diluted in He were introduced into the reactor through heated provisional tubes. The standard H_2O feed concentration employed during steam gasification experiments was equal to 10 vol% H_2O/He, while 5 and 20 vol% H_2O/He mixtures were also examined. Pure CO_2 (Air Liquide) was also used to obtain H_2O/CO_2/He gasifying mixtures of various compositions. The outlet composition was analyzed by an on line gas chromatograph, equipped with TCD/FID detectors [51]. In each gasification experiment, the effluent stream was directed to a cold trap to remove steam and tarry matters prior to their entrance to the Gas Chromatograph. Ash was trapped in the frit and removed mechanically after the end of the experiment.

Results and discussion

Characterization of fuel samples

Solid, liquid and gaseous fractions during char production

The pristine coal employed as fuel in the present study is a lignite coal (LG) from the South field of Ptolemaida-Kozani mines, Western Macedonia, Greece. Lignite chars were obtained via torrefaction at 300 °C (LG300) and slow pyrolysis at 500 °C (LG500) and 800 °C (LG800), as described in Section Char production process. The solid (S), liquid (L) and gaseous (G) products' yields during LG torrefaction and slow pyrolysis, are presented in Fig. 1. Thermal treatment decreases the solid yield from 88 wt.% at 300 °C, to 73.5 wt.% at 500 °C and to 57.7 wt.% at 800 °C. This downward trend can be mostly attributed to the decrease of the organic matter in chars through the devolatilization process and to a minor extent to

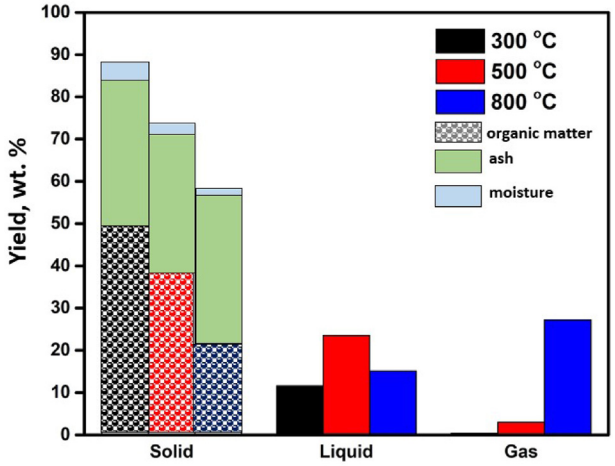

Fig. 1 – Solid (S), liquid (L) and gas (G) yields (wt.%) as a function of thermal treatment of pristine lignite (LG) at 300, 500 and 800 °C. The distribution of the organic matter, moisture and ash in the solid fraction is also depicted in the corresponding bars.

moisture removal upon the increase of treatment temperature (Fig. 1). The latter is further confirmed by the proximate analysis included in Table 1. On the other hand, the yield of gaseous products follows an opposite trend, as it is increased from 3 wt.% at 500 °C to 27.2 wt.% at 800 °C, with negligible gaseous products during torrefaction. The yield to liquid products exhibits a volcano behavior with a maximum value of 23.5 wt.% at 500 °C. The present findings are consistent with relevant literature studies; at low temperatures the solid products (chars) are favored, while high temperatures lead mainly to permanent gas molecules [29,52–55].

Chemical analysis

The chemical composition of pristine lignite (LG) and chars at 300, 500 and 800 °C, namely LG300, LG500 and LG800, respectively, are listed in Table 1. The fixed carbon is increased gradually from 17.96 wt.% over raw LG to 19.12, 21.89 and 25.23 wt.% for LG300, LG500 and LG800 samples, respectively. Similarly, the ash content progressively increased from 40.18 over pristine LG sample to 42.03, 48.79 and 62.97 wt.% for LG300, LG500 and LG800 chars, respectively. On the other hand, the hydrogen, oxygen, volatile matter (VM) and moisture contents decrease steadily upon increasing the thermal treatment temperature (Table 1).

The total sulphur content is decreased from 0.97 wt.% in raw lignite to 0.92 wt.% and 0.68 wt.% in the LG300 and LG500 fuels, respectively, and rises to 0.90 wt.% in LG800 char. The modifications in the sulphur content of different samples are attributed both to the organic sulphur that is released through the devolatilization process upon thermal treatment as well as to the inorganic sulphur in the contained ash [56].

The decrease of the VM content in the lignite chars, which is more pronounced at high thermal treatment temperatures, is attributed to the rapture of the loosely bonded volatile compounds. The latter results in cracks and open pores into fuel's particles, further facilitating the devolatilization step [29,53]. This is in accordance with the pronounced impact of thermal treatment on the surface area and pore volume, as further discussed below. During the torrefaction and slow pyrolysis processes, the removal of aliphatic carbon from the pristine lignite is followed by the removal of aliphatic hydrogen and oxygen, in agreement with the decrease of hydrogen and oxygen contents with treatment temperature (Table 1). The hydrogen content in the as-produced chars is decreased by raising the treatment temperature, principally attributed to the release of unstable groups such as free and self-associated OH groups and aliphatic C–H structures [56,57]. The demonstrated decrease in oxygen can be associated to the breakage of carboxyl, hydroxyl and methoxyl functional groups at elevated temperatures [58]. This downward trend is less prominent for LG, LG300 and LG500 samples. Remarkably, the oxygen content in the case of LG800 char almost eliminates, implying the complete rapture of the aforementioned groups. Notably, in all samples, the fixed carbon content was lower than the overall carbon content denoting that the remaining carbon is still present in the as-produced chars, as volatile matter.

Figure 2 presents the H/C and O/C mass ratios for pristine LG and as-derived chars. Interestingly, an almost monotonic decrease of H/C and O/C ratios is observed upon increasing the temperature of thermal treatment, due to the decomposition of weakly-bonded unstable substances and functional groups [29,58,59]. This trend presumably indicates that thermal treatment improves the maturity of lignite [57]. The latter is further revealed by the calculation of aromaticity factor, f_a, for all samples (Table 1), which was obtained from the expressions provided in Refs. [60–62], on the basis of volatile matter content, carbon content and atomic ratios (H/C, O/C, and O/H), on dry and ash-free basis. The aromaticity factor is monotonically increased with the increase of thermal treatment temperature, reflecting the descending trend of H/C and O/C

Table 1 – Chemical composition and aromaticity of fuels.

	Ultimate analysis[a] (wt.%)					Proximate analysis (wt.%)				Atomic ratios		Aromaticity factor[b]
	C	H	N	O	S	Moisture	Ash[a]	Volatile matter[a]	Fixed carbon[a]	H/C	O/C	f_a
LG	36.22	2.94	1.05	18.63	0.97	7.67	40.18	41.85	17.96	0.97	0.38	0.410
LG300	36.32	2.75	1.05	16.93	0.92	3.36	42.03	38.84	19.12	0.91	0.35	0.440
LG500	35.26	1.75	0.99	12.53	0.68	2.82	48.79	29.31	21.89	0.60	0.27	0.538
LG800	34.01	1.01	0.73	0.37	0.90	0.91	62.97	11.79	25.23	0.36	0.01	0.792

[a] On dry basis.
[b] On dry and ash-free basis.

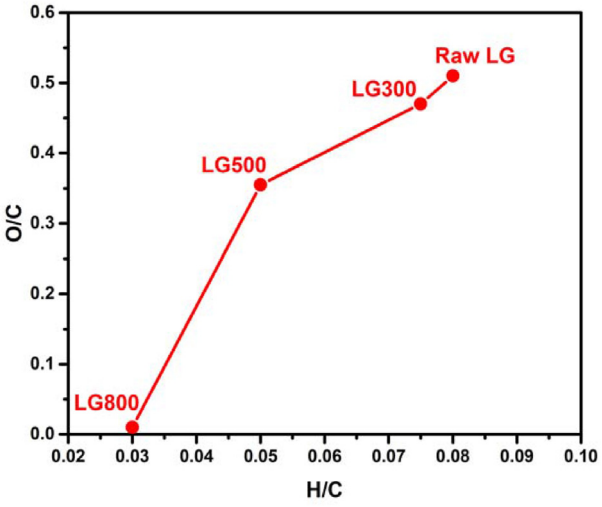

Fig. 2 – H/C and O/C mass ratios of raw lignite and as-produced chars.

atomic ratios. This behavior implies the increase of aromatic carbon atoms in coal upon thermal treatment and thus the enhanced maturity of as-produced chars [62].

Table 2 summarizes the weight concentration of the principal inorganic oxides of the ash contained in LG and lignite chars. The main constituents of ash are SiO_2, CaO and Al_2O_3, followed by lower amounts of Fe_2O_3, SO_3, MgO and Na_2O, while minor quantities of K_2O, TiO_2, P_2O_5 and Cl were also observed. The high calcium content is in line with the limestone soils prevailing in the Western Macedonia region, Greece.

In order to signify the importance of minerals in ash, the alkali index (Al) was calculated, according to the following equation [63–65]:

$$Al = \text{Ash (wt. \%)} \times [(Fe_2O_3 + CaO + MgO + Na_2O + K_2O)/(SiO_2 + Al_2O_3)] \quad (1)$$

As shown in Table 2, the alkali index follows the order: LG800 (51.73) > LG500 (38.62) > LG300 (32.99) > LG (31.53). Taking into account that both the pristine LG sample and chars have a similar ash composition, the increase of alkali index upon thermal treatment can be associated to the increased ash content in chars instead to the different ash composition [66]. A close relationship between the AI and the achieved gasification efficiency is obtained in the present work, implying its key role on gasification process, as further discussed below.

Table 2 – Ash composition (wt.%) and alkali index of fuel samples.

Oxide	LG	LG300	LG500	LG800
Na_2O	2.16	2.18	1.61	1.58
MgO	5.11	5.15	5.04	5.33
Al_2O_3	14.79	14.76	14.96	14.51
SiO_2	34.19	34.33	34.84	33.74
P_2O_5	0.38	0.39	0.41	0.40
Cl	0.02	0.02	0.02	0.02
SO_3	5.86	5.68	3.70	5.09
K_2O	0.96	0.97	0.99	1.00
CaO	30.21	30.23	31.77	31.73
Fe_2O_3	5.19	5.15	5.48	5.45
TiO_2	0.80	0.82	0.83	0.83
Alkali Index (Al)	**31.53**	**32.99**	**38.62**	**51.73**

Textural and morphological analysis

Figure 3 depicts the main textural characteristics of raw LG and chars, in terms of BET area, total pore volume (V_p) and average pore size diameter (d_{av}). BET area increases upon increasing the thermal treatment temperature.

More specifically, the pristine LG exhibits a BET surface area of 7.1 m^2/gr, while the slowly pyrolyzed LG500 and LG800 lignite chars showed values of 19.5 and 190.6 m^2/gr, respectively. The pore structure of the torrefied char (LG300) did not reveal any notable change, compared with the pristine lignite. Subsequently, V_p increases while d_{av} monotonically decreases at temperatures above 300 °C. Similar findings were also obtained by Fanrui Meng et al. [56] and Xiaofei Feng et al. [57], who concluded that the BET area and total pore volume of chars are increased with thermal treatment, being conducive of the fact that the removal of VM and tars during pyrolysis led to the formation of internal porosity.

Figure 4 shows the SEM pictures of the pristine lignite and chars. The corresponding analysis of the LG sample reveals non-uniform particles with a size ranging from 1 to 10 μm. As far as the morphological analysis of the lignite chars is concerned, they exhibit irregular morphology with medium to high polydispersity and 0.7–5 μm sized particles. It can be reasonably assumed by SEM analysis (Fig. 4) that LG300 and LG500 samples possess a more compact pore structure in comparison with LG800 sample. This is in accordance with the improvement of textural properties upon increasing the treatment temperature (Fig. 3).

It has been shown that the different counterparts in the ash could affect in a different extent the gasification process [16,67]. Alkalis, transition and alkaline earth metals were found to catalytically enhance the gasification performance, while silicon, aluminium and Cl exhibit a detrimental effect. In this regard, EDX was employed to obtain the relative atomic surface concentration (at.%) of coal chars (Table 3). The atomic concentration of C is clearly reduced with thermal treatment, coinciding with the decreased trend of carbon content (Table 1). On the other hand, the oxygen atomic composition remains essentially unaffected upon thermal treatment. In this point, the difference between the oxygen content measured by the EDX and ultimate analysis should be mentioned. The latter is ascribed to the fact that ultimate analysis records the elemental oxygen contained in the organic matter and moisture of fuel samples, without taking into account the oxygen bonded to the metallic phases in ash. On the contrary, the oxygen concentration obtained by the EDX measurements corresponds to the overall oxygen contained in the carbonaceous matter, H_2O and metal oxides of the ash [68,69]. Therefore by taking into account the co-current decrease of organic matter and moisture with the increasing share of ash in char samples, upon thermal treatment, the unmodified oxygen content measured by the EDX analysis for all samples can receive a consistent explanation.

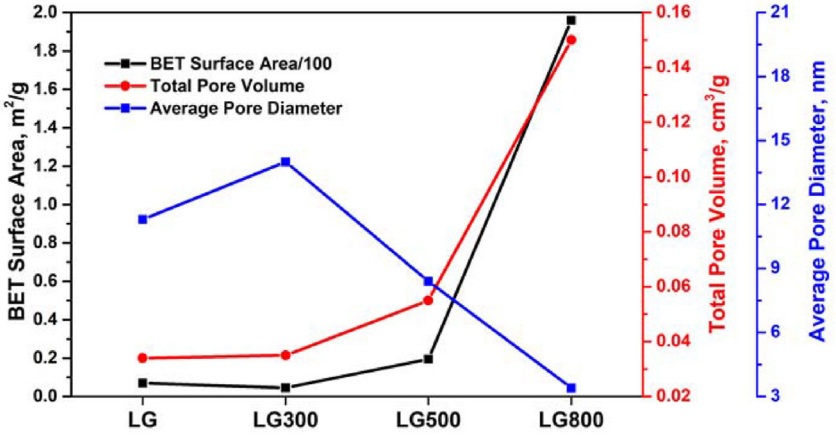

Fig. 3 – Textural properties of pristine lignite and chars.

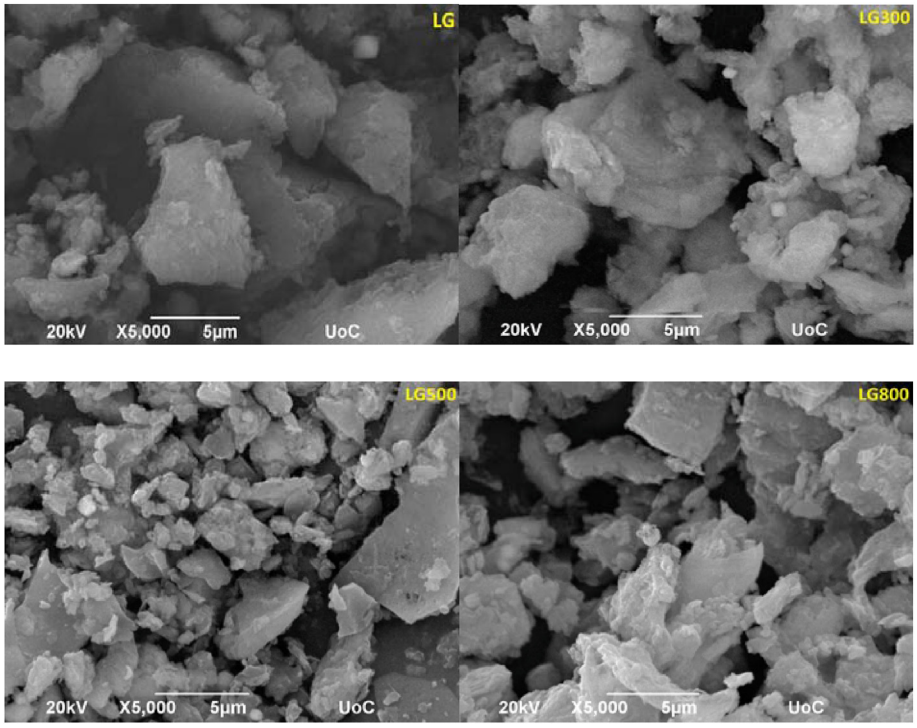

Fig. 4 – SEM micrographs (x5000) of pristine lignite and as-produced chars.

Table 3 – EDX analysis of pristine lignite and as-produced chars.

Samples	Elemental analysis (at.%)						
	C	O	Fe	Ca	Mg	Al	Si
LG	65.1	30	0.17	1.74	0.33	0.73	1.20
LG300	57.9	32.45	0.27	4.25	0.38	1.23	2.33
LG500	58.14	33.19	0.68	2.04	0.36	1.29	3.85
LG800	53.72	31.34	1.05	4.28	1.08	2.39	4.16

LG800 char possesses the highest alkali index (Table 2) and relatively higher atomic surface concentrations of Fe, Ca and Mg, compared to LG, LG300 and LG500, which could further support its enhanced gasification performance (see below). In a similar manner, a pronounced catalytic effect of the aforementioned transition and alkaline earth metals on coal gasification performance has been reported [70–72].

FTIR analysis

The FTIR analysis of the employed fuels are presented in Fig. 5. As revealed by the comparison of the obtained spectra, there are obvious differences spotted mainly in the regions of 3400–3300 cm^{-1}, 1500–1400 cm^{-1} and 1100–1000 cm^{-1}. More specifically, in the wavenumbers range of 3700–3000 cm^{-1}, pristine LG reveals the presence of bands associated to hydroxyl (–OH) groups, which are disappeared on the thermal

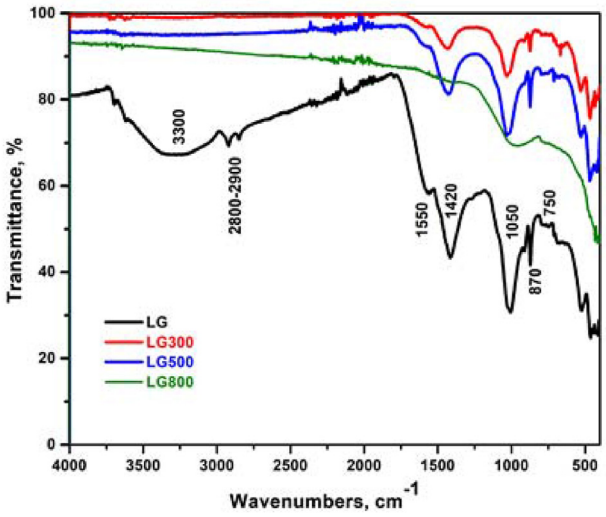

Fig. 5 – FTIR analysis of LG and chars.

treated samples, confirming the very low moisture content of the lignite chars (Table 1). The aliphatic C–H bands of $-CH_2$ and $-CH_3$ groups are noticeable at the 2900-2800 cm^{-1} stretching region in the raw LG sample [73] while these bands are almost absent in chars, in line with their lower volatile matter content and H/C atomic ratio (Table 1). The intensity of the bands appeared at lower wavenumbers (1600–1400 cm^{-1}), which are commonly assigned to aromatic C=C ring stretching vibration, carbonyl, carboxyl, and C=O groups, is decreased upon increasing the temperature of thermal treatment, due to the removal of volatiles and the reorganization of the carbonaceous structure [56,74–78]. The peak at ca. 1000 cm^{-1} is ascribed to C–O stretching in aliphatic ethers and alcohols [56]. The intensity of this peak, which represents oxygenated functional groups, is gradually decreased upon increasing the temperature of thermal treatment.

The bands at ca. 870 and 750 cm^{-1} can be attributed to aromatic structures with isolated hydrogen atoms [79]. The intensity of these bands is diminished in the case of LG800, implying that the aliphatic structures as well as the oxygen-containing groups are decreased upon thermal treatment [78]. This behavior is in agreement with the decreasing trend of H/C and O/C atomic and mass ratios (Table 1, Fig. 2).

Steam gasification performance of raw LG and LG chars

It is generally agreed that coal gasification proceeds through three sequential steps, described below. The principal reactions (R) taking place during coal gasification are listed in Table 4. Initially, the primary devolatilization step of pyrolysis process is taking place at lower temperatures, where the loosely bonded VM is released and a char residue is produced along with the generation of tars, volatiles and non-condensable gases (R1, R2). Then, the secondary devolatilization step and thermal cracking reactions start to prevail, leading to the generation of additional volatiles and tars, which are further decomposed or reformed to H_2, CO_X, CH_4 and light hydrocarbons (R2-R5). In parallel, several partial and complete oxidation reactions involving carbon/char, CO and H_2 (R6-R9) are also taking place. Finally, at higher temperatures, the gasification reactions of the remaining carbonaceous matter (R11-R14) along with C1 and light hydrocarbons steam/dry reforming reactions (R15-R18) are occurring, while the overall reaction network is balanced by the equilibrium of the forward and reverse Water Gas Shift (WGS) stoichiometry (R10).

Figure 6 shows the effect of operation temperature on the concentration (vol%) profiles of the main syngas constituents, namely H_2 (6a), CO_2 (6b), CO (6c) and CH_4 (6d), during steam gasification of LG and char fuels in non-isothermal experiments under batch mode of operation. More specifically, the gasification of LG, LG300 and LG500 fuels is completed at 850–900 °C, while LG800 is totally consumed at 950 °C, in consistency with the order of fixed carbon content (Table 1). The produced synthesis gas mixture is comprised mainly of H_2 and CO_2, followed by CO and minor amounts of CH_4.

The H_2 production profile exhibits an onset temperature at ca. 500 °C with two maxima. The first peak centered at ca. 600–650 °C is assigned to the second step of gasification and coincides for all fuels, while the second maximum, ascribed to the endothermic gasification and reforming reactions, is obtained at 750 °C for LG, LG300 and LG500 samples and shifts to 800 °C for LG800. The first peak can be attributed to the H_2 production through the reactions R2-R5 [20,80,81], with the LG300 and LG500 samples offering the higher H_2 concentration, followed by the pristine LG and LG800 fuels. At high temperatures the R13-R18 endothermic processes are strongly favored and a second maximum for H_2 formation is obtained, following the order LG800 > LG500 ≈ LG300 > LG. This behavior aligns with relevant literature works on coal gasification, using several fuel feedstock such as brown coal, bituminous coal and Shengli lignite [20,82–84].

Regarding CO_2 and CO, all fuels follow the same profile at temperatures up to 600–650 °C. Noticeably, CO_2 and to a lower extent CO exhibit a remarkable production at 300 °C, i.e., during the first step of gasification. According to Butermman et al. [85], thermal cracking at low temperatures breaks down the carbonaceous lattice, resulting in oxygen removal, and in turn on char conversion to CO_X (R6-R8). Carbon dioxide generation, was generally favored at lower temperatures due to the exothermic carbon and CO oxidation reactions (R7 and R8) and the WGS equilibrium (R10). At higher temperatures (>650 °C), CO_2 is sharply decreasing, favoring CO generation, through the endothermic R12, R16 and R18 reactions [53,86], while the final outlet concentrations of CO_2 and CO are mostly dictated by the equilibrium reverse WGS reaction (R10) [87]. In all samples, the CO generation profile coincides with the corresponding hydrogen production curves (Fig. 6a), presenting two peaks located at ca. 650 and 750–800 °C. LG800 due to its higher fixed carbon (Table 1) provides more active sites for the R12 and R13 reactions, which due to their endothermic character are favored at higher temperatures (>650 °C). Overall, the higher CO_2 molar fraction at the effluents

Table 4 – Reaction network during coal gasification.

A/A	Reactions	Process	ΔH°_{rxn} (kJ/mol)
R1	Coal → Volatiles + Char + Tars	Pyrolysis	–
R2	Coal → Tars+CO_2+CO+H_2+CH_4+H_2O+HCs	Primary/Secondary devolatilization	–
R3	Tar → CO_2 + CO + H_2 + CH_4 + HCs	Tar decomposition	–
R4	Tar + H_2O → CO + H_2 + CO_2 + CH_4 + HCs	Steam tar cracking	–
R5	Tar + CO_2 → CO + H_2 + CH_4 + HCs	Dry tar cracking	–
R6	C + ½ O_2 ↔ CO	Partial oxidation	−110.5
R7	C + O_2 → CO_2	Complete oxidation	−393.6
R8	CO + ½ O_2 → CO_2	CO oxidation	−283.5
R9	H_2 + ½ O_2 → H_2O	H_2 oxidation	−285.8
R10	CO + H_2O ↔ CO_2 + H_2	Water Gas Shift (WGS)	−41.2
R11	C + 2H_2 ↔ CH_4	Hydrogasification	−74.9
R12	C + CO_2 ↔ 2CO	Reverse Boudouard	172.5
R13	C + H_2O ↔ CO + H_2	Primary steam gasification	131.3
R14	C + 2H_2O ↔ CO_2 + H_2	Secondary steam gasification	90.2
R15	CH_4 + H_2O ↔ 2CO + 3H_2	Steam methane reforming	206.2
R16	CH_4 + CO_2 ↔ 2CO + 2H_2	Dry methane reforming	247.4
R17	C_nH_m + n H_2O ↔ (n + m/2) H_2 + n CO	Hydrocarbons steam reforming	–
R18	C_nH_m + n CO_2 ↔ m/2H_2 + 2n CO	Hydrocarbons dry reforming	–

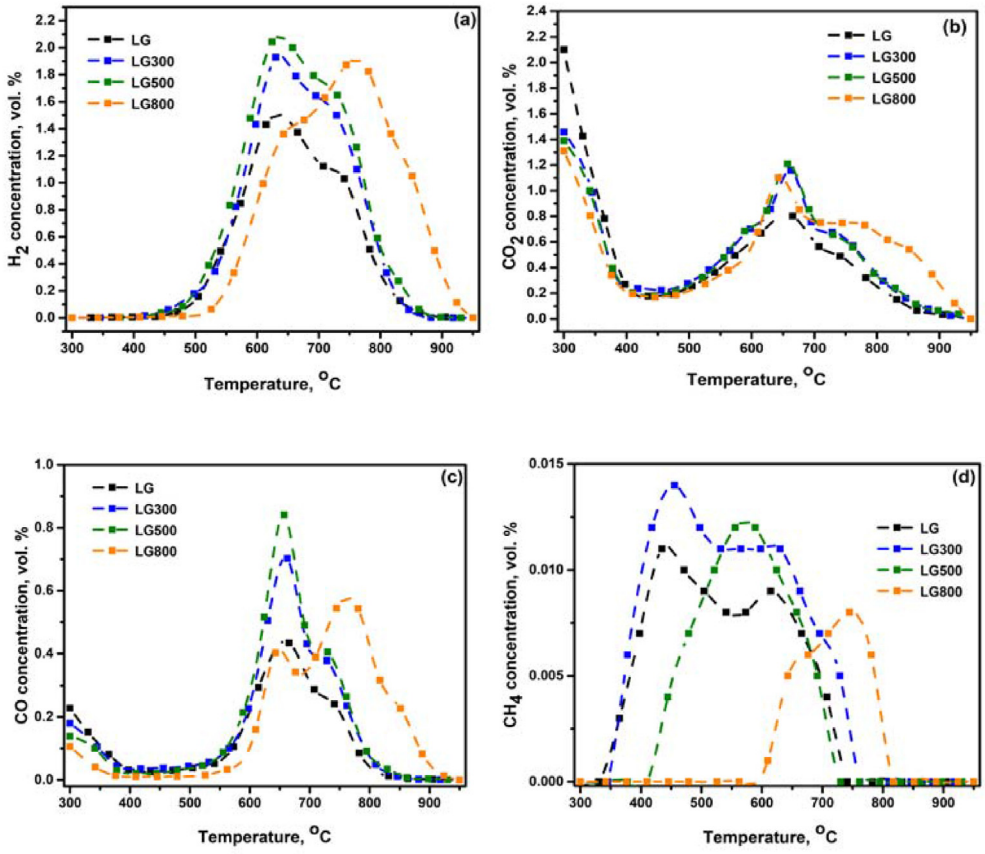

Fig. 6 – Concentration (vol%) profiles of H_2 (a), CO_2 (b), CO (c) and CH_4 (d) in syngas during LG and chars steam gasification. Fuel mass: 100 mg, gasification agent: 10 vol% H_2O/He, flowrate: 30 cm^3/min.

compared to CO is attributed to the enhanced WGS reaction in excess H_2O conditions, in accordance to other research works [83,88–91].

Concerning CH_4, a dual maximum peak at ca. 450 °C and 650 °C is appeared, mostly in LG and LG300 fuels. The low temperature feature corresponds to primary devolitilization, while the high temperature peak is ascribed to secondary devolitilization and thermal cracking processes as well as to exothermic CO_X methanation and hydrogasification (R11) reactions [19]. The thermally treated samples at 500 and 800 °C exhibit only the high temperature peak, in line with their lower VM content (Table 1).

To further elaborate on the reactivity of raw LG and lignite chars (LG300, LG500 and LG800), the carbon-to-gas percent conversion, X (%), the instant gasification rate, R (min^{-1}), and the cumulative syngas products' yields, Y_i (mol), were calculated by employing the following equations [28,72]:

$$X(\%) = \frac{\int_0^t \left[\frac{F_t \cdot \sum_i y_i}{V_M \cdot 100} \cdot MWc\right] \cdot dt}{m_0} \cdot 100, \; with\; i = (CO,\; CO_2,\; CH_4) \quad (2)$$

$$R = \frac{1}{100} \cdot \frac{dX}{dt} \quad (3)$$

$$Y_i = \int_0^t \frac{F_t \cdot y_i}{V_M \cdot 100} \cdot dt, \; with\; i = (H_2,\; CO,\; CO_2,\; CH_4) \quad (4)$$

where F_t is the outlet flowrate of effluents in lt/min, y_{H2}, y_{CO}, y_{CH4}, y_{CO2}, are the molar fractions of H_2, CO, CH_4 and CO_2, respectively. MW_C is the molecular weight of carbon (12 g/mol), V_M is the molecular volume at 298 K and 1 atm (24.436 lt/mol), and m_0 is the initial weight of carbon (gr) introduced in the lab-scale gasifier.

Figure 7 shows the carbon conversion of raw lignite and as-produced chars during steam gasification. For all samples, the carbon conversion increases with the gasification temperature following a sigmoid profile. At temperatures below 450 °C, carbon conversion corresponds to primary devolitilization, generally following the order of the volatile matter content, i.e., LG > LG300 > LG500 > LG800. At the temperature regime of 450–650 °C, where the secondary devolitilization and thermal cracking processes are prevailing, the carbon conversion of LG, LG300 and LG500 is similar (ca. 42%) and slightly higher than that of LG800 (35%). Above this temperature, where the endothermic reactions are favored, significant differences on carbon conversion are obtained.

In particular, the carbon conversion for pristine LG is slowing down from 650 to 800 °C and then levels off up to 950 °C at 77%. On the contrary, the conversion rate of chars was significantly enhanced at higher temperatures. LG300 and LG500 follow a parallel trend, with LG500 exhibiting slightly higher carbon conversion values in the temperature range of 650–800 °C. Then, above 800 °C, the carbon conversion values for both samples are reaching a plateau and remain unchanged up to 950 °C, with X equaled to 88 and 92% for LG300 and LG500 chars, respectively. Interestingly, LG800 exhibits a sharper increase in carbon conversion, surpassing that of the other char samples at temperatures higher than ca. 800 °C, reaching almost complete carbon conversion at 950 °C. Overall, in terms of maximum carbon conversion values at the temperature region where gasification is prominent, the fuels follow the order LG800 > LG500 > LG300 > LG, indicating the beneficial impact of thermal treatment on carbon conversion.

Figure 8 presents the instant gasification rate, R (min^{-1}), for all fuel samples as a function of operational temperature. Below 450 °C, the gasification reactivity can be mainly attributed to primary devolitilization as well as to fuels oxidation by the released oxygenated functional groups. In this temperature region, the reactivity of samples follows the order of volatile matter content, i.e. LG > LG300 > LG500 > LG800, as in the case of carbon conversion (Fig. 7). Above 450 °C, the gasification rates gradually increase with temperature showing a maximum at ca. 680 °C, where the gasification reactivity follows the order: LG500 > LG300 > LG800 > LG, coinciding again with the carbon conversion order at the intermediate temperature regime where secondary devolitilization and thermal cracking reactions are taking place (Fig. 7).

At temperatures higher than 700 °C, the gasification rate of LG, LG300 and LG500 is gradually decreased and almost nullified at 900 °C. However, as in the case of carbon conversion, LG800 exhibits a different behavior. The instant gasification rate of LG800 slightly decreased from 700 to 750 °C and then increased up to 830 °C, in line with the high temperature hydrogen peak (Fig. 6a). Subsequently, the instant gasification rate declined and almost vanished at 950 °C. Therefore, in

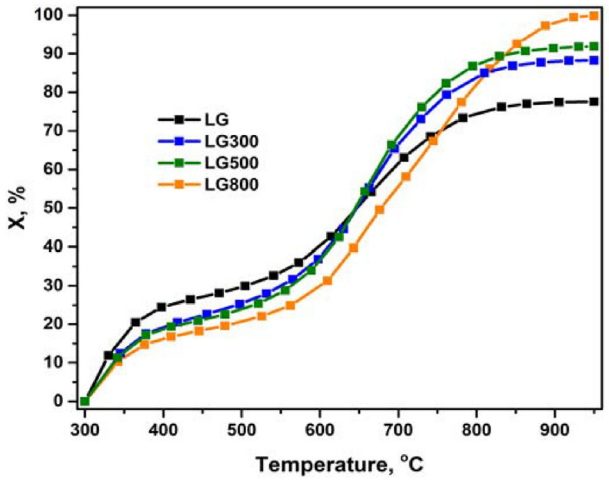

Fig. 7 – The dependence of carbon conversion, X (%) on the operation temperature, for raw LG and as-produced chars during steam gasification. Fuel mass: 100 mg, gasification agent: 10 vol% H_2O/He, flowrate: 30 cm^3/min.

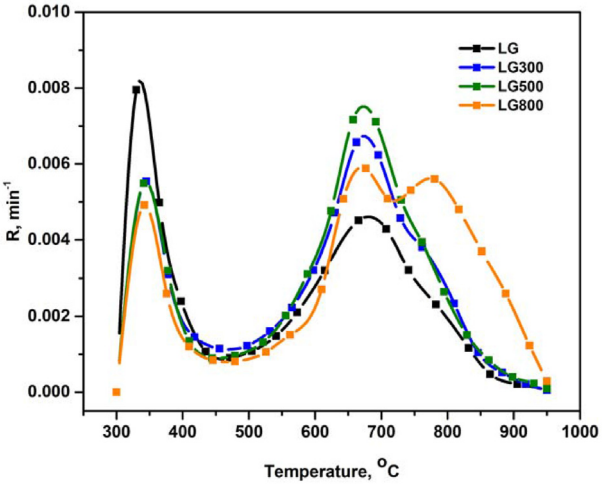

Fig. 8 – Instant gasification rate, R (min^{-1}), versus temperature for raw lignite and as-produced chars during steam gasification. Fuel mass: 100 mg, gasification agent: 10 vol% H_2O/He, flowrate: 30 cm^3/min.

terms of the instant gasification rate, the fuels reactivity at high temperatures coincides with carbon conversion, implying that as the temperature of thermal treatment increases more reactive fuels can be obtained.

Figure 9 illustrates the cumulative products' yields and distribution (Eq. (4)) of the three major gaseous products (H_2, CO, and CO_2) in syngas mixture for raw LG and lignite chars. Methane formation rate is about two orders of magnitude lower compared to the evolution rates of H_2, CO and CO_2 and thus it is not shown for brevity's sake. The total syngas yield is notably enhanced upon thermal treatment following the order: LG800 (55.8 mmol/gr) > LG500 (53.6 mmol/gr) > LG300 (50.1 mmol/gr) > LG (41.6 mmol/gr). The alterations in syngas composition during the raw LG and chars steam gasification is also illustrated in Fig. 9. For the raw lignite, the cumulative molar fractions of H_2 and CO_2 are almost identical (ca. 44%) whereas the corresponding value for CO is four times lower (11.8%). Moreover, it can be observed that as the thermal treatment temperature increases, the CO_2 molar fraction reduces from 44 to 38%, for LG and LG800, respectively, while in turn the H_2 content increases from 43.8 to 49.3%. Interestingly, the differences in CO concentration are less significant.

Based on the above results, it could be claimed that the thermal treatment of Greek lignite (LG) remarkably modifies the physicochemical features of chars, which in turn are directly reflected on the gasification performance. The latter is clearly verified in the present work by the observed modifications on carbon conversion, instant gasification rate, and syngas yield. Notably, the increase of thermal treatment temperature of lignite leads to chars with improved BET surface area and pore volume, higher fixed carbon and ash content. On the other hand, the thermal treatment of LG results in lower volatile matter content as well as in lower H/C and O/C mass/atomic ratios.

Interestingly, the fixed carbon content, ash content, AI and BET area follow in general the same trend as the carbon conversion (Fig. 7), the instant gasification rate (Fig. 8) and the cumulative syngas yields (Fig. 9), i.e., LG800 > LG500 > LG300 > LG, highlighting their essential impact on gasification. The reverse behavior is obtained for H/C and O/C mass/atomic ratios and volatile matter content. These structure-property relationships are clearly demonstrated in Fig. 10, where the effect of the aforementioned factors on total gas yield under steam gasification conditions is represented.

Similar results were observed in the studies of Wei H. et al. [64] and Qinhui Wang et al. [92], who reported that chars with larger BET surface area (S_{BET}) possess higher gasification reactivity under CO_2 or H_2O atmospheres. Moreover, the higher gas yield capacity of chars derived by Shengli lignite (SL) was attributed to their higher fixed carbon content [93]. Jiangdong Yu et al. [19] reviewed the gasification of low-grade coals in sub- and supercritical water. They concluded that as the O/C and H/C ratios decrease along with the increase in fixed carbon content, upon increasing thermal treatment temperature, chars with better gasification performance were obtained. Na Li et al. [28] examined the steam gasification of SL and its demineralized chars. They observed that inherent minerals contained in the ash enhanced the steam gasification reactivity of all examined fuels towards the generation of H_2 and CO_2.

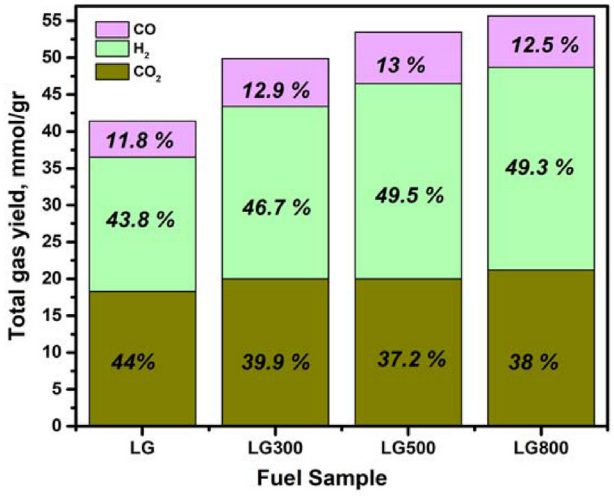

Fig. 9 – Cumulative yields and product distribution (H_2, CO and CO_2) in syngas during steam gasification of LG and chars. Fuel mass: 100 mg, gasification agent: 10 vol% H_2O/He, flowrate: 30 cm^3/min.

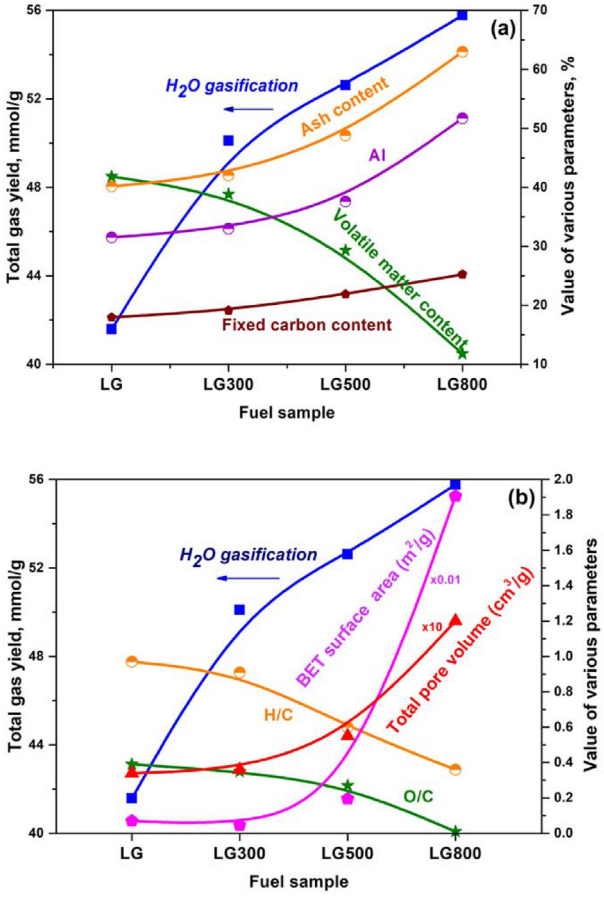

Fig. 10 – Correlation of the total syngas yield with the physicochemical characteristics of raw lignite (LG) and as-produced chars (a, b).

Adjusting the H_2/CO ratio in syngas mixtures

The thermochemical conversion of solid fuels through gasification is of particular importance, taking into consideration the multiple potential uses of syngas [94–96]. Syngas can be employed to produce several commercially important chemicals (i.e., CH_3OH, HCOOH, HCHO, CH_3COOH, DME, olefins, methylamines, gasoline additives, etc) and synthetic gaseous/liquid fuels through the Fischer-Tropsch process. Moreover, it can be directly employed as feedstock in ICEs, gas turbines and fuel cells (i.e., SOFCs, MCFCs) [10,12,14,97,98]. However, a suitable H_2/CO ratio in syngas is required for each application. For example, in the case of methanol and Fischer-Tropsch synthesis the desired H_2/CO ratio equals to 2 [13], while in DME production and oxo-synthesis the ideal H_2/CO ratio is unity [96]. On the other hand, when syngas is directly used as fuel in energy conversion systems (e.g., SOFCs), a higher H_2 content is required towards an increased power generation.

The syngas quality depends strongly on the fuel physicochemical features and the employed operational conditions, with gasifying agent being one of the most decisive parameters. In view of this fact, the employment of CO_2 as gasifying agent has been recently considered as a promising approach to utilize CO_2 captured industrial emissions [99]. Moreover, when replacing steam, CO_2 possesses several advantages such as minimized heat requirements for vaporization, while it can additionally manipulate the H_2/CO ratio in syngas to meet the required specifications for different applications [100].

In view of the above aspects, and in an attempt to tune the H_2/CO ratio in syngas, the effect of CO_2 as an additional gasifying agent to H_2O/He mixtures is explored.

Figure 11 depicts the effect of H_2O:CO_2 molar ratio on H_2 and CO production (mmol/g) as well as on H_2/CO molar ratio, during lignite gasification. When only H_2O is employed as gasifying agent, the increase of steam content from 5 to 20 vol % has a beneficial effect on both H_2 and CO yields, being more pronounced in the case of H_2 generation. More specifically, the H_2 yield is increased from 13.1 mmol/g at 5 vol% H_2O/He to 18.2 and 21.9 mmol/g for 10 and 20 vol% H_2O/He, respectively. The corresponding values for CO yield are 3.5, 4.9, 5.5 mmol/g for 5, 10 and 20 vol% H_2O/He, respectively. This behavior can be attributed to the excess steam, which shifts the equilibrium of gasification and reforming reactions to H_2 and CO production [38,40]. However, it should be noted, that the H_2/CO ratio remains essentially unaffected (3.7–3.9) upon H_2O content variation (5–20 vol%), implying that the overall reaction network is not modified.

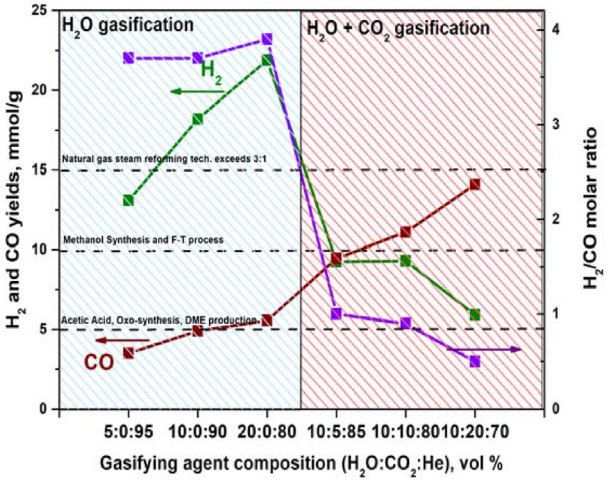

Fig. 11 – Effect of gasifying agent composition on H_2 and CO yields and on syngas H_2/CO ratio during the gasification of raw lignite.

Interestingly, upon gradually co-feeding CO_2 in 10 vol% H_2O/He gasifying mixture, the H_2 and CO production profiles follow opposite trends. In particular, as the CO_2 content increases, the dry gasification and reforming reactions are prevailing resulting in an enhanced formation of CO at the expense of H_2 [101]. The CO yield increases from 9.2 to 11.1 and 14.1 mmol/g for 5, 10 and 20 vol% CO_2 addition in the gasifying agent mixture, respectively. On the other hand, upon CO_2 addition the H_2 yield sharply drops down to approximately 9.3 mmol/g for 5 and 10 vol% CO_2 and to 5.9 for 20 vol% CO_2 concentration, respectively. The present findings are in a good agreement with relevant studies on combined H_2O and CO_2 coal gasification [41,43,101–104].

The aforementioned effect of CO_2 addition on H_2 and CO yields is directly reflected on the H_2/CO ratio, which is substantially decreased in CO_2-containing mixtures, reaching values close to unity in the case of 5 and 10 vol% CO_2, while becoming equal to 0.5 for 20 vol% CO_2. On the basis of the present results, it could be stated that H_2O concentration has a negligible effect on H_2/CO molar ratio, offering H_2/CO ratios as high as ca. 3.8. This limits the potential use of steam gasification syngas in chemical industry. However, upon co-feeding CO_2, the H_2/CO ratio is decreased and depending on the employed CO_2 content in the agent mixture a suitable syngas quality can be obtained for various downstream processes for chemical production [105].

Conclusion

The gasification of low-rank Greek lignite fuel (LG) and its derived chars by thermal treatment at 300, 500 and 800 °C was explored by employing steam as the main gasification agent. Physicochemical characterization of both the pristine lignite and as-produced chars revealed the pronounced effect of thermal treatment on the textural properties, fixed carbon content and alkali index, which then are reflected in the obtained gasification performance. In particular, the total syngas yield is notably enhanced upon thermal treatment, following the order: LG800 (55.8 mmol/gr) > LG500 (53.6 mmol/gr) > LG300 (50.1 mmol/gr) > LG (41.6 mmol/gr). As revealed, the observed gasification yield is proportional to BET surface area, fixed carbon content, and alkali index whereas it is inversely analogous to volatile matter content and to O/C and H/C ratios. Moreover, in an attempt to adjust the H_2/CO ratio of syngas the combination of steam and dry gasification was explored by co-feeding H_2O/CO_2 mixtures as gasifying agents. Interestingly, CO_2 addition drastically decreases the H_2/CO ratio from ca. 3.8 in the case of steam mixtures to values close to unity for H_2O/CO_2 gasifying agent mixtures. The latter is of particular importance in terms of CO_2 utilization and syngas

quality adjustment offering new directions in the field of low-rank carbons upgrade. It should be noted, however, that although LG800 exhibits the best behavior in terms of syngas production, further techno-economic assessment is required; solid yields and energy consumption during char production at different temperature levels should be taken into account towards the optimum fuel choice for practical applications. Work is in progress towards this direction.

Author contribution

A.L. and V.B. contributed to samples preparation and characterization; A.L contributed to gasification studies; G.E.M. and M.K. contributed to the conception, design and results interpretation; G.E.M. and M.K. validated the results and administered the project. A.L. wrote the original draft. Finally, G.E.M. and M.K. reviewed, edited and submitted the manuscript in the final form. All authors contributed to the discussion, read and approved the final version of the manuscript.

Declaration of competing interest

The authors declare that they have no known competing financial interests or personal relationships that could have appeared to influence the work reported in this paper.

Acknowledgements

This research has been co-financed by the European Union and Greek national funds through the Operational Program Competitiveness, Entrepreneurship and Innovation, under the call RESEARCH - CREATE - INNOVATE (project code: T1EDK-01894). The authors are also grateful to Dr. J. Angel Menendéz and Dr. Miguel A. Montes-Morán by the Instituto de Ciencia y Tecnología del Carbono (INCAR-CSIC), Spain, for producing the chars and defining the solid, liquid and gas fractions as well as for providing sufficient amounts of fuels with the desired particle size distribution.

REFERENCES

[1] Prime J. IEA Coal information overview and statistical report. 2019.
[2] Looney B. Statistical review of world energy, 2020. Bp 2020;69:66. 69th ed.
[3] International Energy Agency. Greece 2017 review. Energy Policies IEA Ctries; 2017.
[4] Avagianos I, Violidakis I, Karampinis E, Rakopoulos D, Nanos E, Polonidis N, et al. Thermal simulation and economic study of predried lignite production retrofit of a Greek power plant for enhanced flexibility. J Energy Eng 2019;145:04019001. https://doi.org/10.1061/(asce)ey.1943-7897.0000591.
[5] Karasmanaki E, Ioannou K, Katsaounis K, Tsantopoulos G. The attitude of the local community towards investments in lignite before transitioning to the post-lignite era: the case of Western Macedonia, Greece. Res Pol 2020;68:101781. https://doi.org/10.1016/j.resourpol.2020.101781.
[6] Athens A of. No Title n.d, http://www.academyofathens.gr/el/announcements/press-releases/20200519.
[7] Ahn SY, Eom SY, Rhie YH, Sung YM, Moon CE, Choi GM, et al. Utilization of wood biomass char in a direct carbon fuel cell (DCFC) system. Appl Energy 2013;105:207–16. https://doi.org/10.1016/j.apenergy.2013.01.023.
[8] François J, Abdelouahed L, Mauviel G, Feidt M, Rogaume C, Mirgaux O, et al. Estimation of the energy efficiency of a wood gasification CHP plant using Aspen Plus. Chem Eng Trans 2012;29:769–74. https://doi.org/10.3303/CET1229129.
[9] Grove W. Encyclopedia of materials: science and technology. Solid Oxide Fuel Cells 2001;1–8.
[10] Jewulski J, Skrzypkiewicz M, Struzik M, Lubarska-Radziejewska I. Lignite as a fuel for direct carbon fuel cell system. Int J Hydrogen Energy 2014;39:21778–85. https://doi.org/10.1016/j.ijhydene.2014.05.039.
[11] Li H, Xu N, Fang Y, Fan H, Lei Z, Han M. Journal of Materials Science & Technology Syngas production via coal char-CO2 fluidized bed gasification and the effect on the performance of LSCFN//LSGM. LSCFN solid oxide fuel cell 2018;34:403–8. https://doi.org/10.1016/j.jmst.2017.06.001.
[12] Rady AC, Giddey S, Kulkarni A, Badwal SPS, Bhattacharya S. Catalytic gasification of carbon in a direct carbon fuel cell. Fuel 2016;180:270–7. https://doi.org/10.1016/j.fuel.2016.04.047.
[13] Selvatico D, Lanzini A, Santarelli M. Low Temperature Fischer-Tropsch fuels from syngas: kinetic modeling and process simulation of different plant configurations. Fuel 2016;186:544–60. https://doi.org/10.1016/j.fuel.2016.08.093.
[14] Sun C, Hui R, Roller J. Cathode materials for solid oxide fuel cells: a review. J Solid State Electrochem 2010;14:1125–44. https://doi.org/10.1007/s10008-009-0932-0.
[15] Zabaniotou A, Mitsakis P, Mertzis D, Tsiakmakis S, Manara P, Samaras Z. Bioenergy technology: gasification with internal combustion engine application. Energy Procedia 2013;42:745–53. https://doi.org/10.1016/j.egypro.2013.11.077.
[16] Kaklidis N, Strandbakke R, Arenillas A, Menéndez JA, Konsolakis M, Marnellos GE. The synergistic catalyst-carbonates effect on the direct bituminous coal fuel cell performance. Int J Hydrogen Energy 2019;44:10033–42. https://doi.org/10.1016/j.ijhydene.2019.02.038.
[17] Vamvuka D, Kakaras E, Kastanaki E, Grammelis P. Pyrolysis characteristics and kinetics of biomass residuals mixtures with lignite. Fuel 2003;82:1949–60. https://doi.org/10.1016/S0016-2361(03)00153-4.
[18] Koukouzas N, Katsiadakis A, Karlopoulos E, Kakaras E. Co-gasification of solid waste and lignite - a case study for Western Macedonia. Waste Manag 2008;28:1263–75. https://doi.org/10.1016/j.wasman.2007.04.011.
[19] Yu J, Jiang C, Guan Q, Gu J, Ning P, Miao R, et al. Conversion of low-grade coals in sub-and supercritical water: a review. Fuel 2018;217:275–84. https://doi.org/10.1016/j.fuel.2017.12.113.
[20] Emami Taba L, Irfan MF, Wan Daud WAM, Chakrabarti MH. The effect of temperature on various parameters in coal, biomass and CO-gasification: a review. Renew Sustain Energy Rev 2012;16:5584–96. https://doi.org/10.1016/j.rser.2012.06.015.
[21] Irfan MF, Usman MR, Kusakabe K. Coal gasification in CO_2 atmosphere and its kinetics since 1948: a brief review.

Energy 2011;36:12–40. https://doi.org/10.1016/j.energy.2010.10.034.
[22] Salam MA, Ahmed K, Akter N, Hossain T, Abdullah B. A review of hydrogen production via biomass gasification and its prospect in Bangladesh. Int J Hydrogen Energy 2018;43:14944–73. https://doi.org/10.1016/j.ijhydene.2018.06.043.
[23] Mahishi MR, Goswami DY. An experimental study of hydrogen production by gasification of biomass in the presence of a CO_2 sorbent. Int J Hydrogen Energy 2007;32:2803–8. https://doi.org/10.1016/j.ijhydene.2007.03.030.
[24] Beamish BB, Shaw KJ, Rodgers KA, Newman J. Thermogravimetric determination of the carbon dioxide reactivity of char from some New Zealand coals and its association with the inorganic geochemistry of the parent coal. Fuel Process Technol 1998;53:243–53. https://doi.org/10.1016/S0378-3820(97)00073-8.
[25] Ye DP, Agnew JB, Zhang DK. Gasification of a South Australian low-rank coal with carbon dioxide and steam: kinetics and reactivity studies. Fuel 1998;77:1209–19. https://doi.org/10.1016/S0016-2361(98)00014-3.
[26] Czerski G, Zubek K, Grzywacz P, Porada S. Effect of char preparation conditions on gasification in a carbon dioxide atmosphere. Energy Fuel 2017;31:815–23. https://doi.org/10.1021/acs.energyfuels.6b02139.
[27] Fan D, Zhu Z, Na Y, Lu Q. Thermogravimetric analysis of gasification reactivity of coal chars with steam and CO_2 at moderate temperatures. J Therm Anal Calorim 2013;113:599–607. https://doi.org/10.1007/s10973-012-2838-9.
[28] Li N, Li Y, Ban Y, Song Y, Zhi K, Teng Y, et al. Direct production of high hydrogen syngas by steam gasification of Shengli lignite/chars: remarkable promotion effect of inherent minerals and pyrolysis temperature. Int J Hydrogen Energy 2017;42:5865–72. https://doi.org/10.1016/j.ijhydene.2016.11.068.
[29] Xu Y, Zhang Y, Wang Y, Zhang G, Chen L. Gas evolution characteristics of lignite during low-temperature pyrolysis. J Anal Appl Pyrolysis 2013;104:625–31. https://doi.org/10.1016/j.jaap.2013.05.004.
[30] Zhang SY, Lu JF, Zhang JS, Yue GX. Effect of pyrolysis intensity on the reactivity of coal char. Energy Fuel 2008;22:3213–21. https://doi.org/10.1021/ef800245z.
[31] Zhang Y, Zhang H, Zhu Z, Na Y, Lu Q. Physicochemical properties and gasification reactivity of the ultrafine semi-char derived from a bench-scale fluidized bed gasifier. J Therm Sci 2017;26:362–70. https://doi.org/10.1007/s11630-017-0950-7.
[32] Pinto F, Franco C, André RN, Tavares C, Dias M, Gulyurtlu I, et al. Effect of experimental conditions on co-gasification of coal, biomass and plastics wastes with air/steam mixtures in a fluidized bed system. Fuel 2003;82:1967–76. https://doi.org/10.1016/S0016-2361(03)00160-1.
[33] Xiang Y, Cai L, Guan Y, Liu W, Cheng Z, Liu Z. Study on the effect of gasification agents on the integrated system of biomass gasification combined cycle and oxy-fuel combustion. Energy 2020;206:118131. https://doi.org/10.1016/j.energy.2020.118131.
[34] Singh Siwal S, Zhang Q, Sun C, Thakur S, Kumar Gupta V, Kumar Thakur V. Energy production from steam gasification processes and parameters that contemplate in biomass gasifier – a review. Bioresour Technol 2020;297:122481. https://doi.org/10.1016/j.biortech.2019.122481.
[35] Zhang B, Zhang L, Yang Z, He Z. An experiment study of biomass steam gasification over NiO/Dolomite for hydrogen-rich gas production. Int J Hydrogen Energy 2017;42:76–85. https://doi.org/10.1016/j.ijhydene.2016.10.044.
[36] Skodras G, Nenes G, Zafeiriou N. Low rank coal - CO_2 gasification: experimental study, analysis of the kinetic parameters by Weibull distribution and compensation effect. Appl Therm Eng 2015;74:111–8. https://doi.org/10.1016/j.applthermaleng.2013.11.015.
[37] Veca E, Adrover A. Isothermal kinetics of char-coal gasification with pure CO2. Fuel 2014;123:151–7. https://doi.org/10.1016/j.fuel.2014.01.066.
[38] Fermoso J, Gil MV, García S, Pevida C, Pis JJ, Rubiera F. Kinetic parameters and reactivity for the steam gasification of coal chars obtained under different pyrolysis temperatures and pressures. Energy Fuel 2011;25:3574–80. https://doi.org/10.1021/ef200411j.
[39] Fermoso J, Gil MV, Borrego AG, Pevida C, Pis JJ, Rubiera F. Effect of the pressure and temperature of devolatilization on the morphology and steam gasification reactivity of coal chars. Energy Fuel 2010;24:5586–95. https://doi.org/10.1021/ef100877t.
[40] Wang YG, Chen XJ, Yang SS, He X, Chen ZD, Zhang S. Effect of steam concentration on char reactivity and structure in the presence/absence of oxygen using Shengli brown coal. Fuel Process Technol 2015;135:174–9. https://doi.org/10.1016/j.fuproc.2015.01.016.
[41] Bai Y, Lv P, Yang X, Gao M, Zhu S, Yan L, et al. Gasification of coal char in H2O/CO2 atmospheres: evolution of surface morphology and pore structure. Fuel 2018;218:236–46. https://doi.org/10.1016/j.fuel.2017.11.105.
[42] Roberts DG, Harris DJ. Char gasification kinetics in mixtures of CO_2 and H2O: the role of partial pressure in determining the extent of competitive inhibition. Energy Fuel 2014;28:7643–8. https://doi.org/10.1021/ef502101b.
[43] Chen C, Wang J, Liu W, Zhang S, Yin J, Luo G, et al. Effect of pyrolysis conditions on the char gasification with mixtures of CO_2 and H_2O. Proc Combust Inst 2013;34:2453–60. https://doi.org/10.1016/j.proci.2012.07.068.
[44] Bai Y, Wang Y, Zhu S, Yan L, Li F, Xie K. Synergistic effect between CO_2 and H_2O on reactivity during coal chars gasification. Fuel 2014;126:1–7. https://doi.org/10.1016/j.fuel.2014.02.025.
[45] Jayaraman K, Gökalp I, Jeyakumar S. Estimation of synergetic effects of CO2 in high ash coal-char steam gasification. Appl Therm Eng 2017;110:991–8. https://doi.org/10.1016/j.applthermaleng.2016.09.011.
[46] Wang YL, Zhu SH, Gao MQ, Yang ZR, Yan LJ, Bai YH, et al. A study of char gasification in H_2O and CO_2 mixtures: role of inherent minerals in the coal. Fuel Process Technol 2016;141:9–15. https://doi.org/10.1016/j.fuproc.2015.06.001.
[47] Valin S, Bedel L, Guillaudeau J, Thiery S, Ravel S. CO_2 as a substitute of steam or inert transport gas in a fluidised bed for biomass gasification. Fuel 2016;177:288–95. https://doi.org/10.1016/j.fuel.2016.03.020.
[48] Samaras P, Diamadopoulos E, Sakellaropoulos GP. The effect of mineral matter and pyrolysis conditions on the gasification of Greek lignite by carbon dioxide. Fuel 1996;75:1108–14. https://doi.org/10.1016/0016-2361(96)00058-0.
[49] Kokorotsikos PS, Stavropoulos GG, Sakellaropoulos GP. Effect of catalyst impregnation conditions on Greek lignite hydrogasification. Fuel 1986;65:1462–5. https://doi.org/10.1016/0016-2361(86)90124-9.

[50] Kakaras E, Koukouzas N, Grammelis P, Evaggelos K. Co-gasification of lignite and RDF in Greece laboratory of steam boilers and thermal plants, school of mechanical engineering, national technical university of Athens , Athens , Greece Institute for Solid Fuels Technology and Applications/Centre for R n.d.
[51] Lampropoulos A, Kaklidis N, Athanasiou C, Montes-Morán MA, Arenillas A, Menéndez JA, et al. Effect of Olive Kernel thermal treatment (torrefaction vs. slow pyrolysis) on the physicochemical characteristics and the CO_2 or H_2O gasification performance of as-prepared biochars. Int J Hydrogen Energy 2020. https://doi.org/10.1016/j.ijhydene.2020.11.230.
[52] Radenović A. Pyrolysis of coal. Kem u Ind Chem Chem Eng 2006;55:311–9.
[53] Xu Y, Zhang G, Chen L, Ding X, Zhang Y. Pyrolysis products properties from lignite. Asian J Chem 2013;25:4828–32. https://doi.org/10.14233/ajchem.2013.14116.
[54] Mavridou E, Antoniadis P, Littke R, Lücke A, Krooss BM. Liberation of volatiles from Greek lignites during open system non-isothermal pyrolysis. Org Geochem 2008;39:977–84. https://doi.org/10.1016/j.orggeochem.2008.01.006.
[55] Chattopadhyaya G, Macdonald DG, Bakhshi NN, Soltan Mohammadzadeh JS, Dalai AK. Preparation and characterization of chars and activated carbons from Saskatchewan lignite. Fuel Process Technol 2006;87:997–1006. https://doi.org/10.1016/j.fuproc.2006.07.004.
[56] Meng F, Yu J, Tahmasebi A, Han Y, Zhao H, Lucas J, et al. Characteristics of chars from low-temperature pyrolysis of lignite. Energy Fuel 2014;28:275–84. https://doi.org/10.1021/ef401423s.
[57] Feng X, Zhang C, Tan P, Zhang X, Fang Q, Chen G. Experimental study of the physicochemical structure and moisture readsorption characteristics of Zhaotong lignite after hydrothermal and thermal upgrading. Fuel 2016;185:112–21. https://doi.org/10.1016/j.fuel.2016.07.101.
[58] Yu J, Jiang C, Guan Q, Gu J, Ning P, Miao R, et al. Conversion of low-grade coals in sub-and supercritical water: a review. Fuel 2018;217:275–84. https://doi.org/10.1016/j.fuel.2017.12.113.
[59] Roberts MJ, Everson RC, Neomagus HWJP, Van Niekerk D, Mathews JP, Branken DJ. Influence of maceral composition on the structure, properties and behaviour of chars derived from South African coals. Fuel 2015;142:9–20. https://doi.org/10.1016/j.fuel.2014.10.033.
[60] Gerschel H, Schmidt M. Modelling the relationship between carbon aromaticity of lignite pyrolysis chars and the process temperature with petrographic parameters. Int J Oil Gas Coal Technol 2016;11:290–307. https://doi.org/10.1504/IJOGCT.2016.074769.
[61] Singh KP, Kakati MC. Comprehensive models for predicting aromaticity of coals. Chem Eng Commun 2003;190:1335–47. https://doi.org/10.1080/00986440302148.
[62] Jiang J, Yang W, Cheng Y, Liu Z, Zhang Q, Zhao K. Molecular structure characterization of middle-high rank coal via XRD, Raman and FTIR spectroscopy: implications for coalification. Fuel 2019;239:559–72. https://doi.org/10.1016/j.fuel.2018.11.057.
[63] Sakawa M, Sakurai Y, Hara Y. Influence of coal characteristics on CO_2 gasification. Fuel 1982;61:717–20. https://doi.org/10.1016/0016-2361(82)90245-9.
[64] Huo W, Zhou Z, Chen X, Dai Z, Yu G. Study on CO_2 gasification reactivity and physical characteristics of biomass, petroleum coke and coal chars. Bioresour Technol 2014;159:143–9. https://doi.org/10.1016/j.biortech.2014.02.117.
[65] Koszorek A, Krzesińska M, Pusz S, Pilawa B, Kwiecińska B. Relationship between the technical parameters of cokes produced from blends of three Polish coals of different coking ability. Int J Coal Geol 2009;77:363–71. https://doi.org/10.1016/j.coal.2008.07.005.
[66] Porada S, Czerski G, Grzywacz P, Makowska D, Dziok T. Comparison of the gasification of coals and their chars with CO2 based on the formation kinetics of gaseous products. Thermochim Acta 2017;653:97–105. https://doi.org/10.1016/j.tca.2017.04.007.
[67] Zabaniotou A, Stavropoulos G, Skoulou V. Activated carbon from olive kernels in a two-stage process: industrial improvement. Bioresour Technol 2008;99:320–6. https://doi.org/10.1016/j.biortech.2006.12.020.
[68] Nyakuma BB, Jauro A, Akinyemi SA, Nasirudeen MB, Oladokun O, Bello AA, et al. Physicochemical fuel properties and carbonization kinetics of duduguru coal. Pet Coal 2020;62:1153–62.
[69] Speight JG. Handbook of coal analysis. Handb Coal Anal 2005:1–227. https://doi.org/10.1002/0471718513.
[70] Oboirien BO, Engelbrecht AD, North BC, Eramus RM, Falcon R. Mineral-char interaction during gasification of high-ash coals in fluidized-bed gasification. Energy Fuel 2011;25:5189–99. https://doi.org/10.1021/ef201056j.
[71] Summary E. Influence of mineral matter on the gasification kinetics of coal chars in carbon dioxide stream. Pawe ł Torbus 2015;1–10.
[72] Li Y, Zhou C, Li N, Zhi K, Song Y, He R, et al. Production of high H2/CO syngas by steam gasification of shengli lignite: catalytic effect of inherent minerals. Energy Fuel 2015;29:4738–46. https://doi.org/10.1021/acs.energyfuels.5b00168.
[73] Georgakopoulos A, Iordanidis A, Kapina V. Study of low rank Greek coals using FTIR spectroscopy. Energy Sources 2003;25:995–1005. https://doi.org/10.1080/00908310390232442.
[74] Iglesias MJ, Jiménez A, Laggoun-Défarge F, Suárez-Ruiz I. FTIR study of pure vitrains and associated coals. Energy Fuel 1995;9:458–66. https://doi.org/10.1021/ef00051a010.
[75] Oikonomopoulos I, Th P, Tougiannidis N. FTIR study of two different lignite. Bull Geol Soc Greece 2017;43:2284–93.
[76] Geng W, Nakajima T, Takanashi H, Ohki A. Analysis of carboxyl group in coal and coal aromaticity by Fourier transform infrared (FT-IR) spectrometry. Fuel 2009;88:139–44. https://doi.org/10.1016/j.fuel.2008.07.027.
[77] Georgakopoulos A, Iordanidis A, Kapina V. Study of low rank Greek coals using FTIR spectroscopy. Energy Sources 2003;25:995–1005. https://doi.org/10.1080/00908310390232442.
[78] Ibarra JV, Muñoz E, Moliner R. FTIR study of the evolution of coal structure during the coalification process. Org Geochem 1996;24:725–35. https://doi.org/10.1016/0146-6380(96)00063-0.
[79] Wang S, Tang Y, Schobert HH, Guo Y, Su Y. FTIR and 13C NMR investigation of coal component of late permian coals from southern China. Energy Fuel 2011;25:5672–7. https://doi.org/10.1021/ef201196v.
[80] Ma Z, Zhang SP, Xie DY, Yan YJ. A novel integrated process for hydrogen production from biomass. Int J Hydrogen Energy 2014;39:1274–9. https://doi.org/10.1016/j.ijhydene.2013.10.146.
[81] Cabuk B, Duman G, Yanik J, Olgun H. Effect of fuel blend composition on hydrogen yield in co-gasification of coal and non-woody biomass. Int J Hydrogen Energy 2019;45:3435–43. https://doi.org/10.1016/j.ijhydene.2019.02.130.
[82] Ban Y, Liu Q, Zhou H, He R, Zhi K, Li N. Direct production of hydrogen-enriched syngas by calcium-catalyzed steam

gasification of Shengli lignite/chars: structural evolution. Int J Hydrogen Energy 2020:1–12. https://doi.org/10.1016/j.ijhydene.2020.01.018.
[83] Kim J, Choi H, Lim J, Rhim Y, Chun D, Kim S, et al. Hydrogen production via steam gasification of ash free coals. Int J Hydrogen Energy 2013;38:6014–20. https://doi.org/10.1016/j.ijhydene.2012.12.058.
[84] Kong Y, Kim J, Chun D, Lee S, Rhim Y, Lim J, et al. Comparative studies on steam gasification of ash-free coals and their original raw coals. Int J Hydrogen Energy 2014;39:9212–20. https://doi.org/10.1016/j.ijhydene.2014.04.054.
[85] Butterman HC, Castaldi MJ. CO_2 as a carbon neutral fuel source via enhanced biomass gasification. Environ Sci Technol 2009;43:9030–7. https://doi.org/10.1021/es901509n.
[86] Vélez JF, Chejne F, Valdés CF, Emery EJ, Londoño CA. Co-gasification of Colombian coal and biomass in fluidized bed: an experimental study. Fuel 2009;88:424–30. https://doi.org/10.1016/j.fuel.2008.10.018.
[87] Göransson K, Söderlind U, He J, Zhang W. Review of syngas production via biomass DFBGs. Renew Sustain Energy Rev 2011;15:482–92. https://doi.org/10.1016/j.rser.2010.09.032.
[88] Lu R, Wang J, Liu Q, Wang Y, Te G, Ban Y, et al. Catalytic effect of sodium components on the microstructure and steam gasification of demineralized Shengli lignite char. Int J Hydrogen Energy 2017;42:9679–87. https://doi.org/10.1016/j.ijhydene.2017.01.077.
[89] Huang J, Fang Y, Chen H, Wang Y. Coal gasification characteristic in a pressurized fluidized bed. Energy Fuel 2003;17:1474–9. https://doi.org/10.1021/ef030052k.
[90] Çakal GÖ, Yücel H, Gürüz AG. Physical and chemical properties of selected Turkish lignites and their pyrolysis and gasification rates determined by thermogravimetric analysis. J Anal Appl Pyrolysis 2007;80:262–8. https://doi.org/10.1016/j.jaap.2007.03.005.
[91] Vamvuka D. Gasification of coal. Energy Explor Exploit 1999;17:515–82. https://doi.org/10.1299/jsmemag.62.483_523.
[92] Wang Q, Zhang R, Luo Z, Fang M, Cen K. Effects of pyrolysis atmosphere and temperature on coal char characteristics and gasification reactivity. Energy Technol 2016;4:543–50. https://doi.org/10.1002/ente.201500366.
[93] Yang X, Zhang C, Tan P, Yang T, Fang Q, Chen G. Properties of upgraded shengli lignite and its behavior for gasification. Energy Fuel 2014;28:264–74. https://doi.org/10.1021/ef401497a.
[94] Lee DY, Mehran MT, Kim J, Kim S, Lee SB, Song RH, et al. Scaling up syngas production with controllable H_2/CO ratio in a highly efficient, compact, and durable solid oxide coelectrolysis cell unit-bundle. Appl Energy 2020;257:114036. https://doi.org/10.1016/j.apenergy.2019.114036.
[95] Ravaghi-Ardebili Z, Manenti F, Pirola C, Soares F, Corbetta M, Pierucci S, et al. Influence of the effective parameters on H_2:CO ratio of syngas at low-temperature gasification. Chem Eng Trans 2014;37:253–8. https://doi.org/10.3303/CET1437043.
[96] Cao Y, Gao Z, Jin J, Zhou H, Cohron M, Zhao H, et al. Synthesis gas production with an adjustable H_2/CO ratio through the coal gasification process: effects of coal ranks and methane addition. Energy Fuel 2008;22:1720–30. https://doi.org/10.1021/ef7005707.
[97] Somano V, Ferrero D, Santarelli M, Papurello D. CFD model for tubular SOFC directly fed by biomass. Int J Hydrogen Energy 2021;6. https://doi.org/10.1016/j.ijhydene.2021.02.147.
[98] Lee CG, Kim WK. Oxidation of ash-free coal in a direct carbon fuel cell. Int J Hydrogen Energy 2015;40:5475–81. https://doi.org/10.1016/j.ijhydene.2015.01.068.
[99] Renganathan T, Yadav MV, Pushpavanam S, Voolapalli RK, Cho YS. CO_2 utilization for gasification of carbonaceous feedstocks: a thermodynamic analysis. Chem Eng Sci 2012;83:159–70. https://doi.org/10.1016/j.ces.2012.04.024.
[100] Butterman HC, Castaldi MJ. CO_2 as a carbon neutral fuel source via enhanced biomass gasification. Environ Sci Technol 2009;43:9030–7. https://doi.org/10.1021/es901509n.
[101] Shu X, Li J, Hao J, Liu Z, Wang Q, Lu X. Effect of atmosphere and temperature on syngas production during gasification of Zhundong lignite and water-washed Zhundong lignite in a fixed-bed reactor. Chem Pap 2020;74:555–69. https://doi.org/10.1007/s11696-019-00898-4.
[102] Roberts DG, Harris DJ. Char gasification in mixtures of CO_2 and H_2O: competition and inhibition. Fuel 2007;86:2672–8. https://doi.org/10.1016/j.fuel.2007.03.019.
[103] Tong S, Li L, Duan L, Zhao C, Anthony EJ. A kinetic study on lignite char gasification with CO_2 and H_2O in a fluidized bed reactor. Appl Therm Eng 2019;147:602–9. https://doi.org/10.1016/j.applthermaleng.2018.10.113.
[104] Wang G, Zhang J, Shao J, Liu Z, Wang H, Li X, et al. Experimental and modeling studies on CO_2 gasification of biomass chars. Energy 2016;114:143–54. https://doi.org/10.1016/j.energy.2016.08.002.
[105] Salaudeen SA, Acharya B, Heidari M, Arku P, Dutta A. Numerical investigation of CO_2 valorization via the steam gasification of biomass for producing syngas with flexible H_2 to CO ratio. J CO_2 Util 2018;27:32–41. https://doi.org/10.1016/j.jcou.2018.07.003.